

## OBSERVATIONS AND MODELS OF THE ECLIPSE OF THE CENTRAL STAR OF NGC 2346

R. Costero\*, M. Tapia\*<sup>1</sup>, R.H. Méndez\*\*<sup>2</sup>, J. Echevarría\*, M. Roth\*<sup>1</sup>,  
A. Quintero\*, and J.F. Barral\*

\*Instituto de Astronomía  
Universidad Nacional Autónoma de México

\*\*Instituto de Astronomía y Física del Espacio  
Argentina

Received 1986 August 6

### RESUMEN

Se presentan los resultados del estudio fotométrico que se ha llevado a cabo en el Observatorio Astronómico Nacional en Tonantzintla y San Pedro Mártir, de AGK3-0°965, la estrella central de la nebulosa planetaria bipolar NGC 2346. Se propone un modelo para explicar la mayoría de las observaciones. Este consiste en que los eclipses fueron causados por el paso de una nubecilla de polvo frío cuya forma es elipsoidal, su masa es de  $\sim 10^{-13} M_{\odot}$  y sus dimensiones de  $\sim 2-5 \times 10^{12}$  cm. La velocidad de la nube en la dirección del eje mayor de la órbita proyectada de la binaria central es  $v_p = 0.14 \text{ km s}^{-1}$ , y su componente tangencial en el plano del cielo es  $v_t \sim 3 v_p$ . Otra nube circumestelar más caliente ( $T \lesssim 1000 \text{ K}$ ) es la responsable del exceso infrarrojo observado a longitudes de onda entre 3 y 12  $\mu\text{m}$ ; sus propiedades físicas más relevantes están aún por determinarse y su emisión, vista desde la Tierra, no ha cambiado significativamente en los últimos doce años, como lo muestran las nuevas observaciones aquí reportadas. Los resultados de este trabajo ofrecen la primera evidencia de una nubecilla circumestelar densa, de masa similar a la de un planeta menor y que probablemente es el resultado de la fragmentación de un disco o toroide que gravita alrededor de la estrella central de NGC 2346. Aunque se prevee la existencia de varias otras nubecillas similares en su vecindad, la probabilidad de que en los próximos dos o tres siglos ocurran eventos como el aquí descrito, es muy pequeña.

### ABSTRACT

The photometric behaviour of AGK3-0°965, the central star of the bipolar planetary nebula NGC 2346, has been monitored photometrically for several months at the Observatorio Astronómico Nacional at Tonantzintla and San Pedro Mártir. A model is proposed in which the eclipses were caused by the passage of an ellipsoidal cool dust cloudlet of size  $\sim 2-5 \times 10^{12}$  cm and total dust mass  $\sim 10^{-13} M_{\odot}$ . This model can explain most of the observations. The velocity of the cloud in the direction of the major axis of the projected central binary orbit is  $v_p = 0.14 \text{ km s}^{-1}$ , with a tangential velocity component in the plane of the sky  $v_t \sim 3 v_p$ . Another warmer ( $T \lesssim 1000 \text{ K}$ ) circumstellar cloud is responsible for the infrared excess at wavelengths from 3 to 12  $\mu\text{m}$ . Its emission, as seen from the Earth, has not changed significantly at  $\lambda > 3 \mu\text{m}$  during the past twelve years, as shown by new infrared observations also reported. Its most relevant physical properties are still to be determined. The present results provide the first evidence of a dense circumstellar cloudlet of mass similar to that of a minor planet which is probably the result of the fragmentation of a disk or toroid around the central star of NGC 2346. Although the presence of many other similar cloudlets in its vicinity is expected, the probability of similar events occurring in the next few hundred years is very small.

*Key words:* PLANETARY NEBULAE – PHOTOMETRY – INTERSTELLAR DUST

### I. INTRODUCTION

AGK3-0°965 is the central star of the bipolar planetary nebula NGC 2346. It has been the subject of a large

1. Guest observer, Cerro Tololo Interamerican Observatory, operated by AURA, Inc. for the National Science Foundation.

2. Member of the Carrera del Investigador Científico, CONICET, Argentina. On sabbatical leave at the Institut für Astronomie und Astrophysik der Universität München, Scheinerstrasse 1, 8000 München 80, Federal Republic of Germany.

number of studies in recent years. The main results, prior to 1982, can be summarized as follows:

a) Photometry of the central star was performed by Kohoutek and Senkbeil (1973) giving  $V = 11.12$  and  $B - V = 0.20$ . The magnitude of the star remained constant from 1899 to the end of 1981, as seen in a large collection of archive photographic plates (Schaefer 1983; Luthardt 1983). Méndez (1978) obtained Strömgren photometry and slit spectroscopy of the central ob-

ject; he classified the spectrum of the visible star A5 V and his photometry basically coincided with that of Kohoutek and Senkbeil (1973), implying, in combination with ultraviolet data, a value of  $A_V \approx 0.2$  in the direction of the star.

b) A much higher value of  $A_V \approx 0.8-1.5$  is found from spectroscopy of the planetary nebula itself (Méndez 1978; Méndez and Niemela 1981 and references therein).

c) Since the emission from the visible A-type star could not account for the high excitation of NGC 2346, an undetected companion with  $T_e \approx 10^5$  K was proposed by Kohoutek and Senkbeil (1973) and Calvet and Cohen (1978).

d) The binary nature of AGK3-0°965 was confirmed by Méndez and Niemela (1981) when they obtained a large number of medium resolution spectrograms. They found that the system is a single-line spectroscopic binary with the following parameters: period 15.991 days, systemic velocity of  $25 \text{ km s}^{-1}$  (in agreement with the nebular radial velocity), eccentricity  $e = 0.07$ , mass function  $f(M) = 0.0073 M_\odot$ , and  $a_1 \sin i = 3.6 \times 10^6 \text{ km}$ .

e) Distance determinations for NGC 2346 range from 460 to 1700 pc (Calvet and Cohen 1978; Walsh 1983; Sabbadin 1986; Gathier, Pottasch and Pel 1986 and references therein). In the present work we shall adopt a weighted mean value of 800 pc. An error of even a fac-

tor of two in the adopted value does not affect substantially any of the conclusions of this paper.

f) Near and mid-infrared photometry of the central star was obtained by Cohen and Barlow (1975) and Whitelock (1985) between 1972 and 1981; an infrared excess due to warm ( $T < 1200$  K) dust is evident from their measurements.

Studies of the central star of NGC 2346 made after 1981 have yielded the following results:

a) Kohoutek (1982) discovered large photometric variations with a periodicity similar to that of the binary system.

b) Méndez, Gathier and Niemela (1982) found that the periodic light variations were caused by an eclipse of a dust cloud with extinction characterized by a value of the total to selective absorption  $R = 5-7$ . They also discovered a considerable positive radial velocity excess present only at phases corresponding to minimum light, while otherwise the spectrum of the A5 star remained unchanged at all phases. The eclipse was becoming deeper and broader. These authors proposed a preliminary model in which a large cloud progressively occults the central binary system; the eclipses and radial velocity excesses at minimum light are the result of a high density gradient in the cloud combined with rotation of the visible A star.

c) The evolution of the light curve was further report-

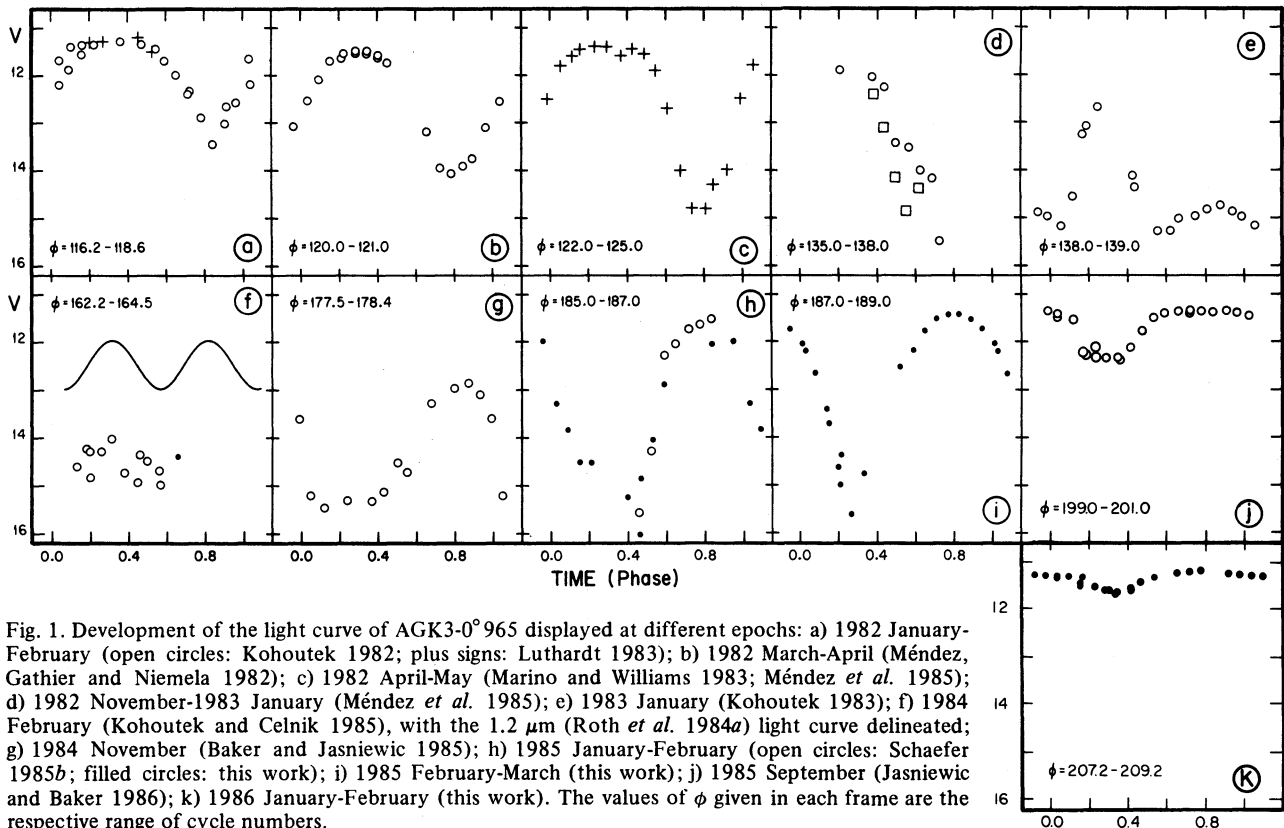


Fig. 1. Development of the light curve of AGK3-0°965 displayed at different epochs: a) 1982 January-February (open circles: Kohoutek 1982; plus signs: Luthardt 1983); b) 1982 March-April (Méndez, Gathier and Niemela 1982); c) 1982 April-May (Marino and Williams 1983; Méndez *et al.* 1985); d) 1982 November-1983 January (Méndez *et al.* 1985); e) 1983 January (Kohoutek 1983); f) 1984 February (Kohoutek and Celnik 1985), with the  $1.2 \mu\text{m}$  (Roth *et al.* 1984a) light curve delineated; g) 1984 November (Baker and Jasniewicz 1985); h) 1985 January-February (open circles: Schaefer 1985b; filled circles: this work); i) 1985 February-March (this work); j) 1985 September (Jasniewicz and Baker 1986); k) 1986 January-February (this work). The values of  $\phi$  given in each frame are the respective range of cycle numbers.

ed by Kohoutek (1983), Méndez *et al.* (1985) and Marino and Williams (1983). By 1983 January, a slight bulge began to develop at the phase of minimum but, at that time, it was regarded as due to possible errors in the subtraction of the contribution of nebular lines (Kohoutek 1983). The development of the light curve from 1982 January to 1983 January is shown in Figure 1*a-e*.

d) A detailed analysis of the properties of the eclipsing cloud and the stellar components was made by Méndez *et al.* (1985). They found certain constraints to the geometry and density distribution of the cloud and suggested, in agreement with Calvet and Peimbert (1983) and Roth *et al.* (1984*a*), that the dust cloud could be a fragment of a disrupted disk toroid which causes the bipolar morphology of the planetary nebula.

e) Ultraviolet observations made with *IUE* by Feibelman and Aller (1983, 1984) confirmed the predictions that the hot subdwarf star would dominate the short wavelength radiation of the system and that the maximum flux of the *UV* CIV and He II lines would occur at phases of minimum visible light, since the A-type and the subdwarf stars are at opposite sides of the orbit.

An extensive study of the light curves in the *JHKL* near-infrared bands was made by Roth *et al.* (1984*a*, hereafter Paper I). There, it was found that the amplitude of the light variations decreases with increasing wavelength with no periodic changes detected at  $\lambda \geq 2 \mu\text{m}$  and that the average absorption (along all phases) at the time of observation, compared to measurements prior to the eclipses (Cohen and Barlow 1975), also decreases with increasing wavelength but was still considerably large ( $A_K \cong 0.4$ ) at  $\lambda = 2.2 \mu\text{m}$ . The development of a secondary maximum 0.5 off phase from the primary maximum was also confirmed.

In Paper I, a two cloud model was proposed in order to explain the observations. One circumstellar warm ( $T \cong 1000 \text{ K}$ ) dust cloud at a radius of a few hundred solar radii dominates the radiation at  $2 \leq \lambda \leq 10 \mu\text{m}$  and another smaller and cool ( $T = 100\text{-}50 \text{ K}$ ) cloud passing at a much larger distance from the central binary, is responsible for the observed eclipses. In order to explain the observed double minima light curve, Méndez *et al.*'s (1985) obscuring dust cloud model was modified in the sense that this cloud should be elongated and tilted some  $25^\circ$  relative to the minor axis of the central star's projected orbit. In Paper I the following prediction was made: "... the secondary maximum (at phase  $\sim 0.8$ ) will dominate the light curve and at the phase of the present primary maximum ( $\sim 0.3$ ), a broad minimum should appear decreasing in width and depth until the eclipse disappears completely..." The disruption of a toroid was adopted as the most plausible origin for the obscuring cloud.

Another interesting model to explain the eclipses of AGK3-0°965 was proposed by Schaefer (1985*a*). He suggested that the near-infrared emitting cloud is responsible for the eclipses and that it was formed by the condensation (just before the eclipses started) of dust

particles out of a clumpy shell of material ejected by the hot subdwarf in the nucleus. This alternative model was attractive because it explained a large number of observations, but cannot be sustained mainly for the following reasons:

1) Unless there are at least 50 similar cloudlets coexisting at roughly the same distance from the hot subdwarf, the condensation of a dust cloud which would have caused the sudden appearance of the eclipse should have been accompanied by a sudden increase in the near-infrared luminosity, especially at  $\lambda = 2\text{-}4 \mu\text{m}$  (see e.g., Williams and Antonopoulou 1979 and references therein); this has not been observed. On the contrary, while the *L*-band magnitude has remained constant since 1974, the luminosity in the *K*-band has decreased as the eclipse progressed.

2) If the obscuring material had been ejected by the hot subdwarf star, it would have done it at a velocity larger than the escape velocity. For the surface gravity of such a star, the escape velocity is at least one order of magnitude larger than the  $70 \text{ km s}^{-1}$  suggested by Schaefer (1985*a*) for the ejected velocity.

In the present work, we present new visual and near-infrared observations of AGK3-0°965, which, combined with all available photometry reported in the literature, are used to determine some of the physical characteristics of the obscuring cloud. The observations and results are presented in the next section; in section III, a discussion on some parameters of the obscuring cloud is given. In section IV we discuss the most likely geometry of such a cloud and in section V, a discussion of our results is given together with a summary of the conclusions. Throughout this work the ephemeris  $2443126.0 + 15.991\text{E}$  (Méndez, Gathier and Niemela 1982) will be used.

## II. OBSERVATIONS AND RESULTS

Johnson's *V*-band photometry of AGK3-0° was made in 1985 and 1986 with the two-channel photometer (for a description, see Nather and Warner 1971) attached to the 1.0-m telescope of the Observatorio Astronómico Nacional (OAN) at Tonantzintla, Puebla, and with the Danish four-channel *uvby* photometer attached to the 1.5-m telescope of the OAN at San Pedro Mártir, Baja California, México; the photometry, on the Ström-gren *y*-band, was converted to Johnson's *V*-band (Cousins and Caldwell 1985). The infrared observations were made with the InSb-based photometers at the 1.5-m telescope of the Cerro Tololo Interamerican Observatory and the 2.1-m telescope of the OAN at San Pedro Mártir (Roth *et al.* 1984*b*). Table 1 shows the log of the observations. The visual results are shown in Table 2 which includes the observed values of the *V*-band magnitudes and those of the star after subtraction of the nebular contribution, which was adopted to be  $V = 14.1$  and  $V = 15.0$  for 20 arcsec and 12 arcsec apertures, respectively. Table 3 gives the available *JHKLM* photometry of AGK3-0°965 at several epochs.

TABLE 1  
VISUAL OBSERVATIONS

Dates	Site	Telescope
1985 January 19 to 1985 March 27	Tonantzintla	1.0-m
1985 December 17 to 1986 February 10	Tonantzintla	1.0-m
1986 January 9 to 1986 February 10	San Pedro Mártir	1.5-m

Local standard stars (Kohoutek 1982): Star A:  $V = 10.24$   
Star B:  $V = 11.02$

NEAR-INFRARED OBSERVATIONS

Date	Site	Telescope
1985 April 14	Cerro Tololo	1.5-m
1986 January 25	San Pedro Mártir	2.1-m
1986 March 21	Cerro Tololo	1.5-m

The results of the present visual photometry are shown as solid circles in Figure 1 which also shows most of the reported photometry at different epochs. Each panel shows the light curve (after subtraction of the nebular contribution) observed at restricted (less than 48 days) intervals along almost six years since the eclipses were discovered. The values of  $\phi$  indicated in each panel are cycle numbers relative to our adopted ephemeris. The continuous sinusoidal line in panel f refers to the shape of the  $J$ -band light curve reported in Paper I. The evolution of the light curve can be described as follows: a narrow eclipse develops between 1981 November and 1982 January ( $\phi = 116$ ) at orbital phase  $\Phi = 0.84$ . The eclipse becomes deeper and broader until a secondary maximum begins to develop at  $\Phi = 0.85$  in 1983 January ( $\phi = 138$ ). Two approximately equal maxima at phases 0.87 and 0.30 are defined in 1984 February ( $\phi = 162$ ) when the average  $A_V$  is highest. The shape of the light curve is shifted 0.5 in phase and by 1984 November ( $\phi = 178$ ), it shows a broad minimum at  $\Phi = 0.26$  and a maximum at  $\Phi = 0.84$ . The minimum becomes narrower at  $\Phi = 0.30$  and, between 1985 March ( $\phi = 187$ ) and 1985 December, it becomes shallower. By 1986 February ( $\phi = 209$ ), the minimum at phase 0.34 is very shallow ( $\leq 0.5$  magnitudes in  $V$ ), indicating that the eclipses have almost ceased.

Figure 2 summarizes the occurrence of the maxima and minima in terms of orbital phase at different epochs. With the exception of a transition interval when the light curve is double-peaked in one period, all maxima (open circles) and minima (filled circles) occur close to phases 0.33 and 0.84 i.e., there is no continuous shifting in phase of the eclipse but a sudden (via the presence of two maxima and minima) 0.5 phase shift occurs; this supports the elongated cloud model with parallel lines of equal absorption tilted at an angle  $\alpha \cong 65^\circ$  relative to

the major axis of the projected binary star orbit (Paper I). Méndez *et al.* (1985) showed that these circumstances lead to a relation between the orbital inclination angle  $i$  and  $\alpha$ :

$$\tan \alpha = B \cos i ;$$

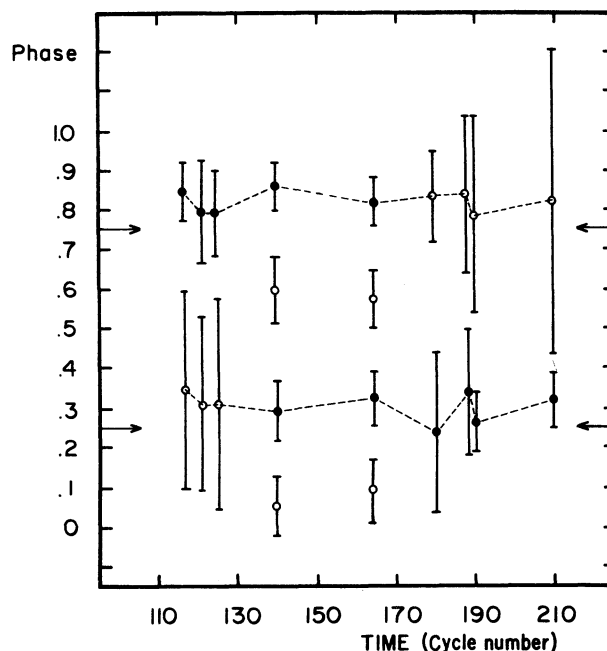


Fig. 2. Phases of the maxima (open circles) and minima (filled circles) as a function of time expressed in cycle numbers. The bars represent the phases during which the star remained within 25% of the flux (in magnitudes) of the corresponding maxima or minima. Horizontal arrows indicate phases 0.25 and 0.75 which correspond to maximum red-shifted and blue-shifted velocity, respectively.

TABLE 2

VISUAL OBSERVATIONS AT THE OBSERVATORIO  
ASTRONOMICO NACIONAL

Julian Date (2440000 +)	Phase	V (obs)	Aperture	Site	V (*)	Julian Date (2440000 +)	Phase	V (obs)	Aperture	Site	V (*)
5760.6	164.76	-	17"	SPM	14.4	6151.65	189.21	13.70	20"	T	14.99
6084.81	185.03	12.87	20"	T	13.29	6417.80	205.10	11.13:	20"	T	11.20:
6085.70	185.09	13.21	20"	T	13.84	6439.80	207.23	11.44	20"	SPM	11.54
6086.74	185.15	13.54	20"	T	14.53	6440.84	207.29	11.50	20"	SPM	11.60
6087.72	185.21	13.55	20"	T	14.55	6441.71	207.35	11.52	20"	SPM	11.63
6091.73	185.46	13.93	20"	T	16.03	6442.88	207.42	11.46	20"	SPM	11.56
6092.76	185.53	13.33	20"	T	14.07	6443.67	207.47	11.34	20"	SPM	11.43
6093.77	185.59	12.59	20"	T	12.90	6444.70	207.54	11.24:	20"	T	11.32:
6106.72	186.40	13.78	20"	T	15.26	6446.65	207.66	11.17	20"	T	11.24
6107.77	186.47	13.67	20"	T	14.88	6447.65	207.72	11.17	20"	T	11.24
6113.72	186.84	11.90:	20"	T	12.05:	6448.66	207.78	11.15	20"	T	11.22
6115.68	186.96	11.86:	20"	T	12.01:	6454.88	208.17	11.28	20"	SPM	11.36
6116.83	187.03	12.03:	20"	T	12.20	6455.80	208.23	11.51	20"	SPM	11.62
6117.65	187.08	12.42	20"	T	12.68	6456.83	208.29	11.55	20"	SPM	11.66
6118.63	187.14	12.95	20"	T	13.41	6457.63	208.34	11.56	20"	SPM	11.67
6119.63	187.20	13.58	20"	T	14.63	6458.80	208.42	11.52	20"	SPM	11.63
6120.62	187.27	13.86	20"	T	15.62	6466.80	208.92	11.19	20"	T	11.27
6121.66	187.33	13.63	20"	T	14.77	6467.75	208.98	11.22	20"	T	11.30
6133.67	188.09	12.40:	20"	T	12.65	6468.76	209.04	11.23	20"	T	11.31
6134.63	188.15	13.17:	20"	T	13.77	6469.74	209.10	11.26	20"	T	11.34
6135.64	188.21	13.48	20"	T	14.38	6470.71	209.16	11.34	20"	T	11.43
6140.75	188.52	12.32	20"	T	12.55	6467.68	208.97	11.27	12"	SPM	11.31
6141.68	188.59	12.03	20"	T	12.20	6468.70	209.03	11.31	12"	SPM	11.35
6142.63	188.65	11.65	20"	T	11.77	6470.73	209.10	11.42	20"	SPM	11.52
6143.70	188.71	11.46	20"	T	11.56						
6144.66	188.77	11.37	20"	T	11.46						
6145.60	188.83	11.37	20"	T	11.46						
6146.60	188.89	11.46	20"	T	11.56						
6147.61	188.95	11.62	20"	T	11.74						
6148.63	189.01	11.90	20"	T	12.05						

TABLE 3

## NEAR-INFRARED OBSERVATIONS

Julian Date	Phase	<i>J</i>	<i>H</i>	<i>K</i>	<i>L</i>	<i>M</i>	Reference
≤ 2442415	-	10.7	9.84	8.64	7.14	-	Cohen & Barlow (1975)
2443873 ≤ JD ≤ 2444970	-	10.65	9.93	8.79	-	-	Whitelock (1985)
2445760.65 (max.)	164.76	11.93	10.55	9.06	7.16	-	Roth <i>et al.</i> (1984a)
2445739.74 (mean)	163.45	12.12	10.65	9.11	7.17	-	Roth <i>et al.</i> (1984a)
2445766.77 (min.)	165.14	12.50	10.82	9.10	7.22	-	Roth <i>et al.</i> (1984a)
2446108.8	186.53	12.20	10.56	9.08	7.4	-	Schaefer (1985b)
2446169.71	190.34	12.02	10.46	9.02	7.31	6.18	This work
2446455.80	208.23	10.59	9.88	8.84	6.99	-	This work
2446510.50	211.62	10.44	9.82	8.83	7.32	-	This work

where the value of the constant B depends on the phases of equal brightness in any instantaneous light curve. At different epochs, the value of B changed with a mean value of  $\sim 3$ . This is not surprising since local inhomogeneities are expected in several parts of the cloud. With a value of  $\alpha = 65^\circ$ , mean values of the inclination angle are  $45^\circ - 60^\circ$ , in agreement with Méndez *et al.* (1985).

The development of the light curve of AGK3-0°965 can be better analysed by studying the values of the total visual extinction  $A_V$  (after subtraction of the pre-eclipse  $A_V = 0.2$ ) at certain fixed orbital phases as a function of time. This would be equivalent to examining the system with a stroboscopic light that "freezes"

the binary to a certain phase. Figure 3 shows plots of  $A_V$  versus time, expressed in cycle number, at four different orbital phases; also, the mean  $A_V$  defined as  $1/2 [A_V(\text{max}) + A_V(\text{min})]$  is shown for each epoch. For comparison, the extinction at K, where no orbital variations are observed, is also plotted.

As expected for a symmetrical passing cloud, the mean visual absorption curve is approximately symmetric in shape with the highest  $A_V$  near the midpoint between the onset and end of the eclipses. This behaviour is similar for the absorption in the K-band, at least for  $\phi \geq 160$ , supporting the conclusion that the emitting near-infrared circumstellar cloud is much larger than the

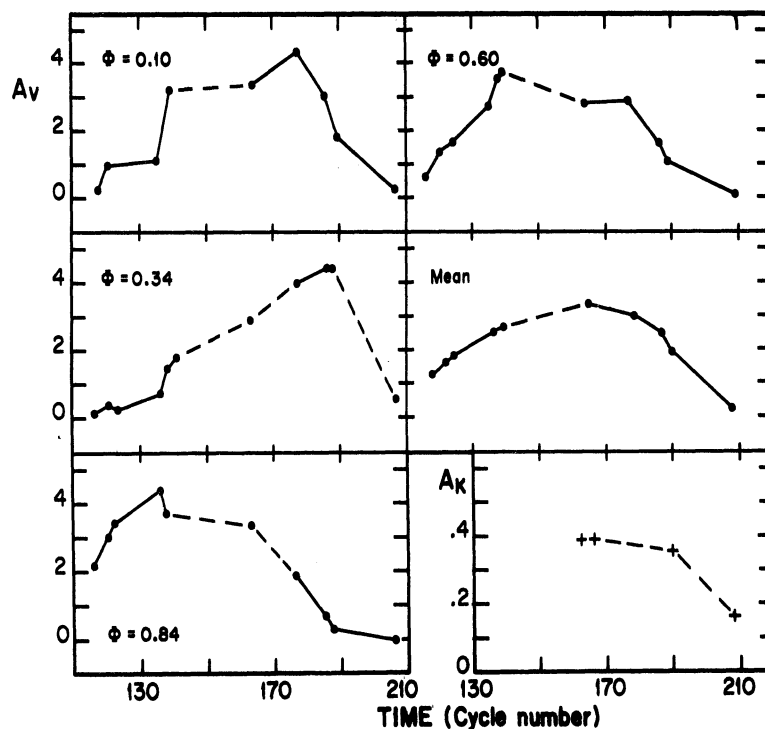


Fig. 3. The total absorption  $A_V$  (in the  $V$  photometric band, after subtraction of the pre-eclipse  $A'_V = 0.2$ ) expressed in magnitudes at four different phases  $\Phi$  and the mean of all phases (see text) as function of time. The absorption in the  $K$ -band ( $2.2 \mu\text{m}$ ) is given in the lower right panel. The estimated error of each  $A_V$  is  $< 0.2$  mag (mainly due to errors in the subtraction of the nebular contribution) and  $\lesssim 0.05$  mag in  $A_K$ . The units in the abscissa are number of cycles after JD 2443126.0 assuming a period of 15.991. The magnitudes prior to eclipses were assumed to be  $V = 11.12$  and  $K = 8.65$ .

obscuring cloud (see Paper I). Nevertheless, the behaviour of the absorption curves at phases 0.84 (where the eclipses began) and 0.34 (where the eclipses ended) is not consistent with a symmetrical cloud moving along the major axis of the projected binary orbit. At  $\Phi = 0.84$  the absorption increases very rapidly and peaks at cycle number 136 (1982 November) but decreases at a much slower rate. At the opposite side of the binary orbit, at  $\Phi = 0.34$ , the situation is drastically different, with the absorption increasing slowly and decreasing sharply after a maximum  $A_V$  at cycle number 188 (1985 February). At intermediate phases (0.1 and 0.6) the differences are not so radical but the mirror-symmetry is also evident. Independently of small scale clumpiness of the obscuring cloud, its overall geometry should give rise to this behaviour.

### III. OVERALL PARAMETERS OF THE OBSCURING CLOUD

The analysis of the behaviour of the light curve of the central star of NGC 2346 favours a picture of an obscuring cloud which is similar to that proposed in Paper I, modified to explain in detail most of the newly available observational data. The dimension of the near-in-

frared emitting cloud and the radius of the A-star orbit should be modified from those given in Paper I. As pointed out by Schaefer (1985a), the dust particles cannot survive the ultraviolet radiation of the hot subdwarf star at a distance of  $\sim 100 R_\odot$  and the minimum radius of this warm dust structure should be  $\sim 500\text{--}1000 R_\odot$ , though the precise distance at which the condensed dust particles would approach equilibrium depends on the radius of the hot star, the composition of the dust particles and their mean size. On the other hand, the radius of the A-star orbit,  $a_1$ , in km, is approximately  $(3.6 \times 10^6)/\sin i$ , that is  $a_1 \approx 4.7 \times 10^6$  km for  $i \approx 50^\circ$  or  $a_1 \approx 7 R_\odot$ .

We can estimate the projected distance travelled by the densest part of the obscuring cloud in the direction of the binary orbit. The major axis of the latter ( $\sim 10^7$  km) was covered in  $848 (\pm 32)$  days, which is the time span between the maximum obscuration at phase 0.84 to the maximum obscuration at phase 0.34. This gives a value of the projected velocity,  $v_p = 0.14 \text{ km s}^{-1}$ . If this velocity is constant, then the width of the cloud in this direction is given by  $H_{AV} = \Delta t_{AV} v_p - 2R_*$ , where  $\Delta t_{AV}$  is the time span between two points where the total absorption  $A_V$  has a certain "threshold" value and  $R_*$  is the radius of the A-type star. Therefore,  $H_0$  would

be the total width in the direction of the projected binary orbit of the cloud measured from the point where  $A_V$  (and hence the column density) is just becoming larger than zero to the point where it comes back to the same value. From Figure 3,  $\Delta t_0 = 1631 (\pm 32)$  days and therefore, for  $R_* = 1.8 R_\odot = 1.3 \times 10^6$  km (Allen 1973),  $H_0 = 1.7 \times 10^7$  km. Probably a more sensible definition of the borders of the elongated cloud would be that for which the mean  $A_V$  is 50% of the maximum value, i.e.,  $A_V = 1.7$ . Then, the effective width is  $H_{1.7} \approx 1.2 \times 10^7$  km.

The column density,  $N_d$  of the dust cloud is related to the visual absorption (in magnitudes) by the formula  $A_V = 1.086 Q_V \pi b^2 N_d$ , where  $Q_V$  is the extinction coefficient and  $b$  is the mean radius of the grains. At maximum obscuration ( $A_V \approx 4$ ), and for  $Q_V = 2.1$  and  $b = 0.2 \mu\text{m}$ ,  $N_d = 1.4 \times 10^9 \text{ cm}^{-2}$ . Assuming that the depth of the cloud is the same as its effective width  $H_{1.7}$ , then  $n_d = 1.2 \times 10^{-3} \text{ cm}^{-3}$  which for (large) grains of mass  $3 \times 10^{-14}$  g, gives a mean density of cloud of  $\bar{\rho}_d = 3.5 \times 10^{-17} \text{ g cm}^{-3}$ . The rather large mean dust density derived above, suggest that the cloudlet is probably self-gravitating.

#### IV. MORPHOLOGY OF THE OBSCURING CLOUD

The overall behaviour of the light curve, from beginning to end of the eclipses, allows us to put some constraints on the shape of the dust cloud and on the path followed by the binary orbit behind the cloud. The spherical model proposed by Méndez *et al.* (1985) and the elongated cloud travelling parallel to the major axis of the projected binary orbit proposed in Paper I, fail to explain the detailed behaviour of the light curve, because if the cloud were spherical (with radial density gradient), no combination of linear path and orientation of the binary orbit would explain the asymmetries of the absorption curves (Figure 3) and the constraints established by Méndez *et al.* (1985) that the motion of the binary relative to the cloud should be roughly parallel to the lines of equal absorption.

As a first approximation, let us analyse an elongated cloud or disk seen edge-on with all isocrypts (lines of equal extinction) parallel to the borders of the cloud and whose velocity vector, relative to the binary orbit, has a component of considerable magnitude perpendicular to the major axis of the projected orbit. As pointed out by Méndez *et al.* (1985), this explains the rather large density gradient implied by the radial velocity excess at minimum light (at  $\phi = 122$ ) and the comparatively slow development of the light curve (Figure 1). Let us consider this model in greater detail. Figure 4 describes graphically the event. There, the boundaries of the obscuring cloud are defined by  $H_0$  and the positions of the major axis of the binary orbit at seven different times are indicated. These are:  $t_0$ ,  $t_6$  are the times when the eclipse began and ended, respectively, at phase 0.84;  $t_1$  is the time when the absorption was maximum at phase 0.84;

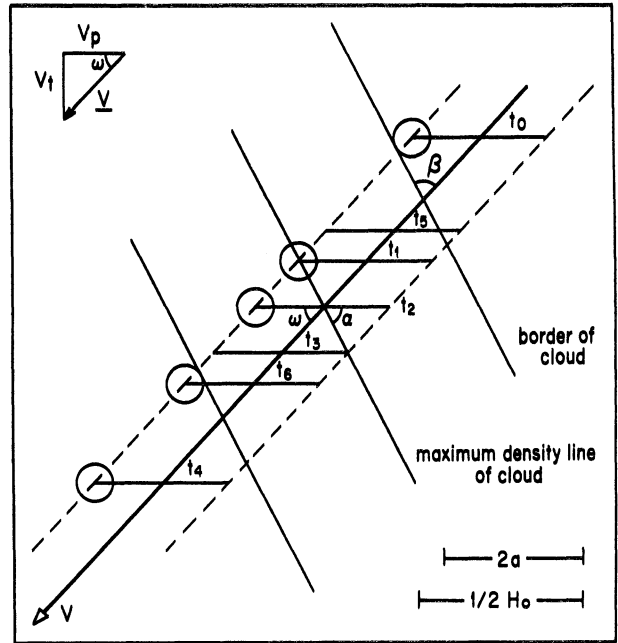


Fig. 4. Analysis of the path of the centre of mass of the binary system and the major axis of the orbit of the A-type star, as seen from the observer's position. Seven positions are indicated, corresponding to times  $t_0$ ,  $t_1$ ,  $t_2$ ,  $t_3$ ,  $t_4$ ,  $t_5$  and  $t_6$ , as defined in the text. The A-star is illustrated at phase 0.75.

$t_2$  is the time of maximum mean (all phases) absorption;  $t_3$  when the absorption is maximum at phase 0.34; and  $t_5$ ,  $t_4$  when the eclipse began and ended, respectively, at phase 0.34. From the geometry of the passage of the dust cloud in front of the binary system as indicated in Figure 4, it can be shown that

$$\omega + \alpha + \beta = 180^\circ,$$

$$\begin{aligned} (t_4 - t_2)/(t_3 - t_1) &= (t_2 - t_0)/(t_3 - t_1) = \\ &= (1/2 H_0 + a_1 + R_*)/(2a_1) \end{aligned} \quad (1)$$

and

$$(t_1 - t_0)/(t_6 - t_1) = 1 = (t_3 - t_5)/(t_4 - t_3); \quad (2)$$

where  $a_1$  is the semi-major axis of the A-star orbit, assumed to be  $5 \times 10^6$  km ( $i \approx 50^\circ$ ),  $R_*$  is the radius of the A-star ( $1.3 \times 10^6$  km) and  $H_0$  is as defined and computed in section III. The right-hand side of equation (1) gives 1.6 which differs from the value obtained from the left-hand terms of the same equation, which give a value of 1.0. The disagreement is still greater for equa-

tion (2) which merely states that the absorption at phases 0.83 and 0.33 should be symmetric in time. It can be clearly seen in Figure 3 that this is not the case for any specific phase, although the mean (overall phases) absorption in  $V$  is indeed symmetric. Furthermore, the absorption curves at phases 0.84 and 0.34 have a mirror symmetry. These facts led us to modify slightly some assumptions for the cloud; mainly that concerning the parallelism of the isocrypts at certain critical phases. An ellipsoidal cloud or tilted disk, like that shown in Figure 5, satisfies nearly all geometrical conditions raised by the observational history of the eclipse, in particular the times involved in the asymmetric absorption curves shown in Figure 3, the existence of two similar minima at phases 0.1 and 0.6 at cycle number 163, the near-constancy of the angles  $\alpha$ ,  $\beta$ , and  $\omega$  (see Figure 4), the different slopes of the ascending and descending branches of the absorption curves (Figure 3) at phases 0.34 and 0.84 and the fact that the minimum at cycle number 186 was deeper than the minimum at cycle number 135.

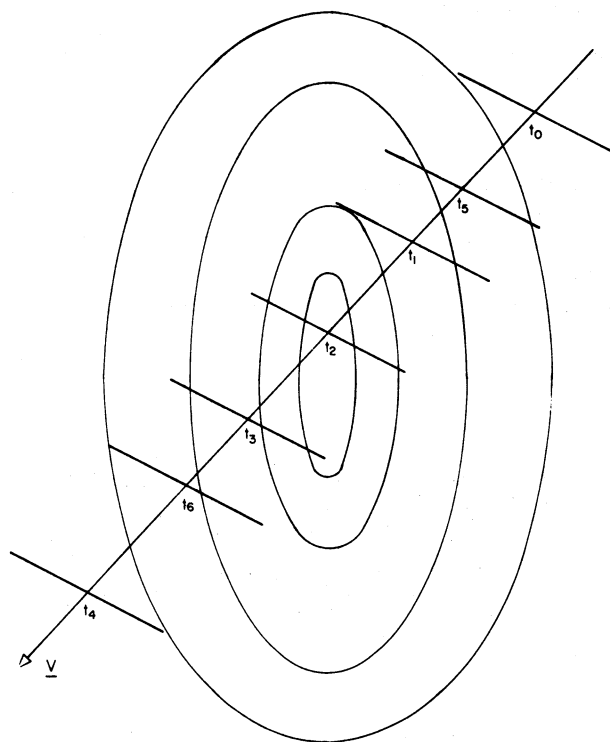


Fig. 5. Schematic representation of the path followed by the binary system relative to the obscuring cloud, as seen from the observer's position. The morphology of the cloud explains the development of the light curve along the duration of the eclipses. The arrow is the path of the centre of mass, the ellipses represent the isocrypts of the proposed cloud, with density increasing towards the centre and the tilted straight lines represent the major axis of the A-star orbit at different epochs, as defined in the text. For this particular example,  $\alpha = 63^\circ$ ,  $\beta = 43^\circ$ ,  $\omega = 74^\circ$  and  $v = 0.5 \text{ km s}^{-1}$ .

The latter is a consequence of the fact that the path of the centre (densest part) of the cloud does not intersect the centre of mass of the binary system but passes closer to the position of the A-star at phase 0.34.

## V. DISCUSSION AND CONCLUSIONS

The extraordinary phenomenon of the eclipse of the central binary system of NGC 2346 by an elongated cloud raises at least two important questions, namely: Is the obscuring dust cloud physically related to NGC 2346 and if so, what is its origin? What fraction of the total amount of dust seen in the far-infrared (*IRAS*) in NGC 2346 corresponds to the proposed absorbing cloudlet?

In the computation of the physical parameters of the cloud (section III), we have assumed that it is located at the same distance as NGC 2346. In fact, the probability that the eclipses were being caused by a very small "field" interstellar cloud is practically nil while there is strong evidence of the presence of large quantities of molecules and dust associated with NGC 2346 (e.g. Méndez and Niemela 1981; Huggins and Healy 1986). It seems only reasonable to think that the obscuring cloud is physically related to the planetary nebula. Let us assume that the velocity ( $v_{\text{orb}}$ ) of the obscuring cloud relative to the centre of mass of the central binary star is some four times the measured component ( $v_p$ ) along the major axis of the binary's projected orbit in the plane of the sky and that it represents the orbital motion of the cloudlet around the central binary star, i.e.,  $v_{\text{orb}} = 4 v_p$ . From Kepler's law,

$$r = GM_T / v_{\text{orb}}^2$$

where  $r$  is the radius of this orbit,  $M_T$  the total mass of the binary system (the mass of the cloudlet is negligible) and  $G$  the gravitational constant. For  $M_T = 3.1 M_\odot$  (Calvet and Peimbert 1983) and  $v_{\text{orb}} \cong 0.5 \text{ km s}^{-1}$ ,  $r = 1.7 \times 10^{17} \text{ cm} \cong 11000 \text{ AU} \cong 0.05 \text{ pc}$ . This radius is within a factor of three of the projected distance from the visible central star to the borders of the well delineated waist of the bipolar planetary nebula. This result, together with the high density of the observed cloudlet, supports the suggestion by Calvet and Peimbert (1983) and Méndez *et al.* (1985) that the obscuring cloud is a fragment of a disrupted toroid which is orbiting around the central binary star. The rather low ( $0.5 \text{ km s}^{-1}$ ) value of the magnitude of the velocity component perpendicular to the binary orbital plane may be the result of the dynamical processes which led to the fragmentation of the toroid.

The 12 to  $100 \mu\text{m}$  measurements of NGC 2346 by the Infrared Astronomical Satellite (*IRAS*) have been analysed by Pottasch *et al.* (1984). They derived a mean dust temperature of  $\sim 50 \text{ K}$ , a total far-infrared flux of  $13 L_\odot$  and a total dust mass  $M_{\text{tot}}^d = 2.5 \times 10^{-4} M_\odot$  (for  $d = 800 \text{ pc}$ ). This value of the mass of dust can explain (within the uncertainties) the local nebular extinc-



tion observed by Méndez and Niemela (1981) and implies that only a very small fraction of the total dust mass ( $M_{\text{c}\ell}^{\text{d}}/M_{\text{tot}}^{\text{d}}$ ) forms the eclipsing cloudlet. In section III we determined a mean density  $\bar{\rho} = 3.5 \times 10^{-17} \text{ g cm}^{-3}$ ; assuming the volume of the ellipsoidal cloud to be

$$V = (4/3) \pi (H_{1.7})^2 (2 H_{1.7}) = (8/3) \pi H_{1.7}^3 = \\ = 1.5 \times 10^{37} \text{ cm}^3,$$

which yields

$$M_{\text{c}\ell}^{\text{d}} \cong 5 \times 10^{20} \text{ g} = 2.5 \times 10^{-13} M_{\odot},$$

then

$$M_{\text{c}\ell}^{\text{d}} / M_{\text{tot}}^{\text{d}} \cong 10^{-9}$$

The total mass (dust plus gas) of the above cloudlet cannot be computed because the dust-to-gas ratio in it is not known; in fact, this ratio should be much larger than the "normal" interstellar value as the gas would have to be dissipated by the cloud's internal pressure in a previous evolutionary phase.

In summary, we have analysed the development of the light curve of the central star of NGC 2346 from the onset to the apparent end of the eclipses and the most important conclusions are:

1) A model of eclipses by the passage of an ellipsoidal cloud can explain almost all observations. The main parameters of the proposed cloud are:  $\bar{\rho}(\text{dust}) \cong 3.5 \times 10^{-17} \text{ g cm}^{-3}$ , dimensions of the three axes of  $\sim 2.5 \times 10^{12} \text{ cm}$  and total dust mass of  $\sim 10^{-13} M_{\odot}$ . The velocity of the cloud in the direction of the major axis of the projected central binary star orbit is  $v_p = 0.14 \text{ km s}^{-1}$  with a tangential velocity component  $v_t$  in the plane of the sky of  $v_t \sim 3 v_p$ . If this passing cloudlet were orbiting with Keplerian motion around the central binary system, the radius of the orbit would be  $\sim 0.04 \text{ pc}$ , with a period of  $\sim 7 \times 10^5 \text{ years}$ . It should be pointed out that the mass of the proposed cloudlet is similar to that of a minor planet. Given the fact that the derived mean density and morphology of the cool cloud suggest that it is probably self-gravitating, then NGC 2346 may represent the first evolved stellar object where planetary bodies are suspected of being formed.

2) If the dust toroid which gives rise to the bipolar morphology of the planetary nebula were indeed in a state of disruption and considering the small fraction of the total dust mass (as derived by *IRAS*) which went into the eclipsing cloudlet ( $\sim 10^{-9}$ ), then we would expect the presence of other similar cloudlets distributed around the minor axis of the nebula. However, the probability of the occurrence of similar eclipsing events in the next few hundred years is rather small. Never-

theless, the long-term monitoring of this object is very important.

Two observational tests to the present model can be performed in the near future: 1) Since the orbital radius of the hot subdwarf, relative to the centre of mass, is larger than that of the A-star, the periodic eclipses of the former should continue and be observable in the 1000 -2000 Å wavelength range. 2) The K (2.2  $\mu\text{m}$ ) magnitude of the central star (observed with an aperture of a few arc seconds) should continue to get brighter as the outer parts of the warm cloud are still being eclipsed, until it becomes completely uncovered.

The assistance of the staff of the Observatorio Astronómico Nacional is acknowledged. RHM is grateful to the Alexander von Humboldt Foundation (F.R.G.) for a Research Fellowship at the Institut für Astronomie und Astrophysik der Universität München. Dr. M.T. Ruiz and Mr. M.A. Rojas helped with some of the observations. We also thank E. Themsel, C. Harris, M.A. García and A. García for their assistance in the preparation of the manuscript. This work was partially supported by a grant from CONACYT (México), No. PCCBBNA-022688. This is Contribution No. 215 of Instituto de Astronomía, UNAM.

#### REFERENCES

- Allen, C.W. 1973, *Astrophysical Quantities* (London: The Athlone Press).
- Baker, A. and Jasiewicz, G. 1985, *Astr. and Ap.*, **143**, L1.
- Calvet, N. and Cohen, M. 1978, *M.N.R.A.S.*, **182**, 687.
- Calvet, N. and Peimbert, M. 1983, *Rev. Mexicana Astron. Astrof.*, **5**, 319.
- Cohen, M. and Barlow, M.J. 1975, *Ap. J. (Letters)*, **16**, 165.
- Cousins, A.W.J. and Caldwell, J.A.R. 1985, *Observatory*, **105**, 134.
- Feibelman, W.A. and Aller, L.H. 1983, *Ap. J.*, **270**, 150.
- Feibelman, W.A. and Aller, L.H. 1984, in *Future of Ultraviolet Astronomy Based on Six Years of IUE Research*, *NASA Conference Publ.* No. 2349, p. 159.
- Gathier, R., Pottasch, S.R., and Pel, J.N. 1986, *Astr. and Ap.*, **157**, 171.
- Huggins, P.J. and Healy, A.P. 1986, *M.N.R.A.S.*, **220**, 33p.
- Jasiewicz, G. and Baker, A. 1986, *Astr. and Ap.*, **160**, L1.
- Kohoutek, L. 1982, *Inf. Bull. Var. Stars*, No. 2123.
- Kohoutek, L. 1983, *M.N.R.A.S.*, **204**, 93p.
- Kohoutek, L. and Celnik, W.E. 1985, *Inf. Bull. Var. Stars*, No. 2759.
- Kohoutek, L. and Senkbeil, G. 1973, *Mem. Soc. Roy. Scie. Liège, 6e. Serie*, **5**, 485.
- Luthardt, R. 1983, *Inf. Bull. Var. Stars*, No. 2360.
- Marino, B.F. and Williams, H.O. 1983, *Inf. Bull. Var. Stars*, No. 2266.
- Méndez, R.H. 1978, *M.N.R.A.S.*, **185**, 647.
- Méndez, R.H. and Niemela, V.S. 1981, *Ap. J.*, **250**, 240.
- Méndez, R.H., Gathier, R., and Niemela, V.S. 1982, *Astr. and Ap.*, **116**, L5.
- Méndez, R.H., Marino, B.F., Clariá, J.J., and van Driel, W. 1985, *Rev. Mexicana Astron. Astrof.*, **10**, 187.
- Nather, R.E. and Warner, B. 1971, *M.N.R.A.S.*, **152**, 209.
- Pottasch, S.R., et al. 1984, *Astr. and Ap.*, **138**, 10.
- Roth, M., et al. 1984a, *Astr. and Ap.*, **137**, L9. (Paper I).

Roth, M., Iriarte, A., Tapia, M., and Reséndiz, G. 1984*b*, *Rev. Mexicana Astron. Astrof.*, 9, 25.  
Sabbadin, F. 1986, *Astr. and Ap.*, 64, 579.  
Schaefer, B.E. 1983, *Inf. Bull. Var. Stars*, No. 2281.  
Schaefer, B.E. 1985*a*, *Ap. J.*, 297, 245.

Schaefer, B.E. 1985*b*, *IAU Circular* No. 4047.  
Walsh, J.R. 1983, *M.N.R.A.S.*, 202, 303.  
Whitelock, P. 1985, *M.N.R.A.S.*, 213, 59.  
Williams, P.M. and Antonopoulou, E. 1979, *M.N.R.A.S.*, 187, 183.

José Barral, Rafael Costero and Alfonso Quintero: Instituto de Astronomía, UNAM, Apartado Postal 70-264, 04510 México, D.F., México.

Juan Echevarría, Miguel Roth and Mauricio Tapia: Instituto de Astronomía, UNAM, Apartado Postal 877, 22860 Ensenada, Baja California, México.

Roberto H. Méndez: Instituto de Astronomía y Física del Espacio, C.C. 67, Suc. 28, 1428 Buenos Aires, Argentina.